Seasonal Morphological Variations and Age-Related Changes of the Seminal Vesicle of Viscacha (*Lagostomus maximus maximus*): An Ultrastructural and Immunohistochemical Study

EDUARDO M. CHAVES,[1]* CLAUDIA AGUILERA-MERLO,[1] ALBANA CRUCEÑO,[1]
TERESA FOGAL,[2] RAMÓN PIEZZI,[2] LUIS SCARDAPANE,[1]
AND SUSANA DOMINGUEZ[1]

[1]Cátedra de Histología, Facultad de Química, Bioquímica y Farmacia, Universidad
Nacional de San Luis, Av. Ejército de los Andes 950-Bloque I, 1° Piso,
5700 San Luis, Argentina
[2]Instituto de Histología y Embriología (IHEM), Facultad de Ciencias Médicas,
Universidad Nacional de Cuyo, CONICET, 5500 Mendoza, Argentina

ABSTRACT

The viscacha is a seasonal rodent that exhibit an annual reproductive cycle with periods of maximum reproductive activity and gonadal regression. We studied seasonal variations in the morphology and cellular population of the seminal vesicles (SVs) during both periods and in impuber animals. Seminal vesicles were studied by light and electronic microscopy. Measurements of epithelial height, nuclear diameter, luminal diameter, and muscular layer were performed. Also, we studied the distribution of androgen receptors (AR) in this gland during the reproductive cycle and in impuber animal. During gonadal regression, principal and clear cells showed signs of reduced functional activity. These were characterized by an epithelium of smaller height, irregular nuclei, and cytoplasm with few organelles, dilated cisterns, and glycogen granules. In impuber animals, the principal cells showed large nuclei with chromatin lax and cytoplasm with small mitochondria, poorly developed Golgi apparatus, and granules of glycogen. On the other hand, the cells exhibited seasonal variations in the distribution and percentage of immunolabeled cells to AR throughout the annual reproductive cycle. During the gonadal regression period, glandular mucosa exhibited numerous epithelial cells with intense nuclear staining. However, fibromuscular stromal cells were weakly positive for AR in contrast to what was observed during the activity period. Considering that testosterone values are lower in adult animals during the period of gonadal regression and in impuber animals, our immunohistochemical results show a significant correlation with the percentage of AR-immunopositive cells. In conclusion, these results demonstrate that the structure of the SVs changes in the activity period of viscacha, probably because of elevated levels of

INTRODUCTION

The seminal vesicles (SVs) are accessory glands of the male reproductive system that synthesize and release an abundant amount of fluids to favor the transport and nutrition of spermatozoids as well as the formation of a vaginal stopper in some rodents.

The morphology of the SVs varies across species. In humans, horse, and rat, they are saccularly shaped, in pig and bull they are compact and multilobulated (Dellman, 1993; Badia et al., 2006), and in some rodent species they exhibit a branched tubular structure (Mollineau et al., 2009; Ayres de Menezes et al., 2010). In cat, marsupials, cetaceans, and some insectivorous primates, the SVs are absent (Setchell et al., 1994; Strzezek et al., 2000).

The SVs, like much of the male reproductive tract, depend on androgen action for normal development and differentiation as well as for later structure and functional integrity (Luke and Coffey, 1994; Thompson, 2001). The active form of the androgen, dihydrotestosterone (DHT), is a potent androgenic metabolite produced in the prostate and SVs by the reduction of testosterone (T) by the action of a specific enzyme, 5α-reductase. The action of androgens on their gland cells depends on the specific binding to an androgen receptor (AR) and the formation of a DHT–AR complex. It has been demonstrated that blocking androgen action impairs male reproductive development, so that males are born with a female phenotype with intraabdominal testes and without prostate and SVs (Welsh et al., 2006). Androgen action in SVs is thought to be predominantly regulated by DHT rather than T because SV stromal cells express 5α-reductase type 2, which converts T to DHT, and 5α-reductase knockout mice have smaller SVs and prostates (Mahendroo et al., 2001).

Few studies have been performed on the accessory glands of the male reproductive system in wild animals with seasonal reproduction. The physiology and behavior of these animals vary throughout the year depending on response to the environmental signals such as length of photoperiod, temperature, rainfall regime, food availability, and social interactions (Demas et al., 2004; Meyer et al., 2006). The photoperiod constitutes the main synchronizer of the adaptive and reproductive characteristics of wild animals (Garidou et al., 2003). The light signal is processed by retinal photoreceptors and transmitted by a multisynaptic neural circuit to the pineal gland, transducing the nervous signal into a hormonal response, mainly melatonin.

Our experimental model is the viscacha (*Lagostomus maximus maximus*), a wild nocturnal South American rodent (Llanos and Crespo, 1954; Jackson, 1989; Jackson et al., 1996). Studies performed in our laboratory have shown that this rodent has seasonal reproduction, the photoperiod being the main synchronizer of the reproductive cycle throughout the year (Dominguez et al., 1987; Fuentes et al., 1993; Mohamed et al., 2000; Filippa et al., 2005). In its habitat, the adult male undergoes a reproductive cycle mainly characterized by a period of higher gonadal activity in the summer and beginning of autumn and lower gonadal activity during the winter (Muñoz et al., 1997, 2001). Thorough studies performed in testes (Muñoz et al., 1998), epididymis (Fuentes et al., 1991; Aguilera-Merlo et al., 2005a, 2009), and spermatozoids of viscacha (Aguilera-Merlo et al., 2005b) have provided important knowledge on the reproductive biology of this rodent. On the other hand, the accessory glands of this species include prostatic gland, the SVs, the coagulating gland, and the bulbourethral glands. However, there are no studies describing the morphological variations in the SVs of this species in relation with the seasonal cycle and age.

The objectives of this work were to describe the morphological characteristics of the SVs of the adult viscacha with relation to its annual reproductive cycle and natural photoperiod. We also determined the serum testosterone levels in different stages of reproductive cycle and in relation to age. On the other hand, we studied the location of ARs by immunohistochemistry for this gland during both periods and in impuber animals.

MATERIALS AND METHODS

Animals

Twelve adult male viscachas (*Lagostomus maximus maximus*) weighing 5–7 kg were captured in their habitat near San Luis, Argentina (33° 20′ south latitude 760 m altitude), between the years 2008 and 2010 using the traps placed in their burrows. Six animals were captured during the reproductive period in summer (February–March), and six animals were captured during the gonadal regression period in winter (July–August). Also, six male animals with body weight between 2 and 3.5 kg were captured during summer and confirmed as impuber according to light microscopy observations of testis (Branch et al., 1993). The animals were anesthetized intramuscularly with a combination of ketamine (Ketamina 50; Holliday-Scott SA®) and xylazine (Vetanarcol®; König SA) at a dose of 12 and 0.4 mg/kg, respectively. The blood was collected for cardiac puncture for the evaluation of serum hormone concentrations and quickly sacrificed by decapitation. The reproductive condition of all animals was carefully assessed based on morphological testes parameters using light microscopy. In San Luis, summer days have 14 hr of light with an average temperature of 25°C. In winter, the light phase decreases to 10 hr and the average temperature is 10°C. The average rainfall is 400 mm in summer and 18 mm in winter. These values were provided by the Servicio Metereológico Nacional

(www.smn.gov.ar). Appropriate procedures were performed to minimize the number of animals used and suffering. The experimental design was approved by the local Ethics Committee and was in agreement with the guidelines of the National Institute of Health (NIH, USA) for the use of experimental animals. Moreover, the Biodiversity Control Area of the Environment Ministry of San Luis (Argentina) approved a study protocol to carry out scientific research within the territory of this province (Resolution No. 03 PRN-2011).

Tissue Samples

The right SV was surgically removed and sliced into 2–3 mm cross-sectional slabs. For light microscopic evaluation, the samples were fixed in Bouin's solution, dehydrated in an increasing ethanol series, and embedded in paraffin. For electronic microscopy evaluation, small blocks ($2 \times 2 \times 2$ mm^3) were obtained from these segments and were fixed in glutaraldehyde–formaldehyde (Karnovsky, 1965) in phosphate buffer. They were postfixed in cold 2% OsO4, dehydrated in an increasing acetone series, and embedded in Spurr's resin. One-micrometer-thick sections were cut with a Porter-Blum ultramicrotome and dyed with toluidine blue for study under the light microscope. Ultrathin sections were stained with uranyl acetate and lead citrate and were observed under an electron microscope (Zeiss EM 900 AG, Oberkochen, Germany). Concomitantly, testicular morphology was evaluated to confirm gonadal activity.

Morphometric Analysis

For each animal, 30 transverse sections of gland were randomly chosen. Measurements were made with a calibrated micrometer ocular using an objective of 25× and 40× (total magnification, 250× and 400×, respectively). Measurements of epithelium height, luminal diameter, and thickness of the muscular layers were performed in paraffin sections.

A computer-assisted image analysis system was used to measure the percentage of immunoreactive cells in SVs, the major cellular and nuclear diameters. The system consisted of a binocular microscope at magnification 200× (Olympus BX-40, PA), interfaced with a computer hosting the image processing and recording system. The images were captured by a digital camera (Sony SSC-DC5OA) and processed with Image Pro Plus software (5.0, Media Cybernetics, Bethesda, MD). The software allowed the following processes: image acquisition, automatic analogous adjusts, thresholding, background subtraction, distance calibration and diameter measuring, and diskette data logging. Images were displayed on a color monitor, and the parameters were measured with the image analysis system. The major cellular and nuclear diameters were measured for each cell with a visible nucleus.

Serum Testosterone Levels

Blood samples were incubated at 4°C for 30 min, centrifuged at 5,000g for 5 min and serum removed, and stored at −20°C. Serum testosterone levels were quantified using the total testosterone test. This is a solid-phase competitive chemiluminescent enzyme immunoassay run on a Siemens* Medical IMMULITE* 1000 Immunoassay Analyzer (Siemens Medical Solutions Diagnostics).

Immunohistochemistry

The tissue sections were first deparaffinized with xylene and rehydrated with decreasing concentrations of ethanol. They were incubated for 20 min in a solution of 3% H_2O_2 in water to inhibit endogenous peroxidase activity. They were then rinsed with distilled water and phosphate-buffered saline (PBS, 0.01 M, pH 7.4). Nonspecific binding sites for immunoglobulins were blocked by incubation for 20 min with normal goat serum diluted in PBS containing 1% bovine serum albumin, 0.09% sodium azide, and 0.1% Tween-20. Sections were then incubated overnight in a humidified chamber at 4°C with the rabbit polyclonal antibody AR (N-20; Santa Cruz Biotechnology). After rinsing with PBS for 10 min, the immunohistochemical visualization was carried out using the Biotin-Streptavidin Amplified system (B-SA) included in the Super Sensitive Ready-to-Use Immunostaining Kit (BioGenex, San Ramon, CA) at 20°C. The B-SA was used as follows: sections were incubated for 30 min with diluted biotinylated anti-mouse IgG, and after being washed in PBS, they were incubated for 30 min with horseradish peroxidise (HRP)-conjugated streptavidin, and finally washed in PBS. The reaction site was revealed by incubation with HRP substrate solution (100 μL 3,3′-diaminobenzidine tetrahydrochloride chromogen solution in 2.5 mL PBS and 50 μL H_2O_2 substrate solution). The sections were subsequently dehydrated and mounted.

To confirm the specificity of the immunoreaction, adjacent sections were stained according to the protocol described above, but lacking incubation with the primary antibody. In additional control, normal rabbit serum was used instead of the primary antibody. No positive structures or cells were found in these sections.

The percentage of immunoreactive cells in SVs in each image was determined. The number of immunoreactive cells (A) and the number of nuclei in unstained cells (B) were counted ($A/(A + B) \times 100$).

Statistics

Means and standard errors were calculated for all data sets. Statistical analyses were performed using a Student's t-test. A value of $P < 0.05$ was accepted as significant.

RESULTS
Morphological Studies

The viscacha SV was found to be paired, elongated, and tortuous in shape. Both glands emptied independently into the urethral light. These glandular tissues were tubular glands formed by three radially arranged histological layers: mucosa, muscular, and adventitia. This epithelium is constituted by three cellular types: principal cells (P), basal cells (B), and clear cells (Cl). The P cells are the most abundant cell population, reaching ~90% of total.
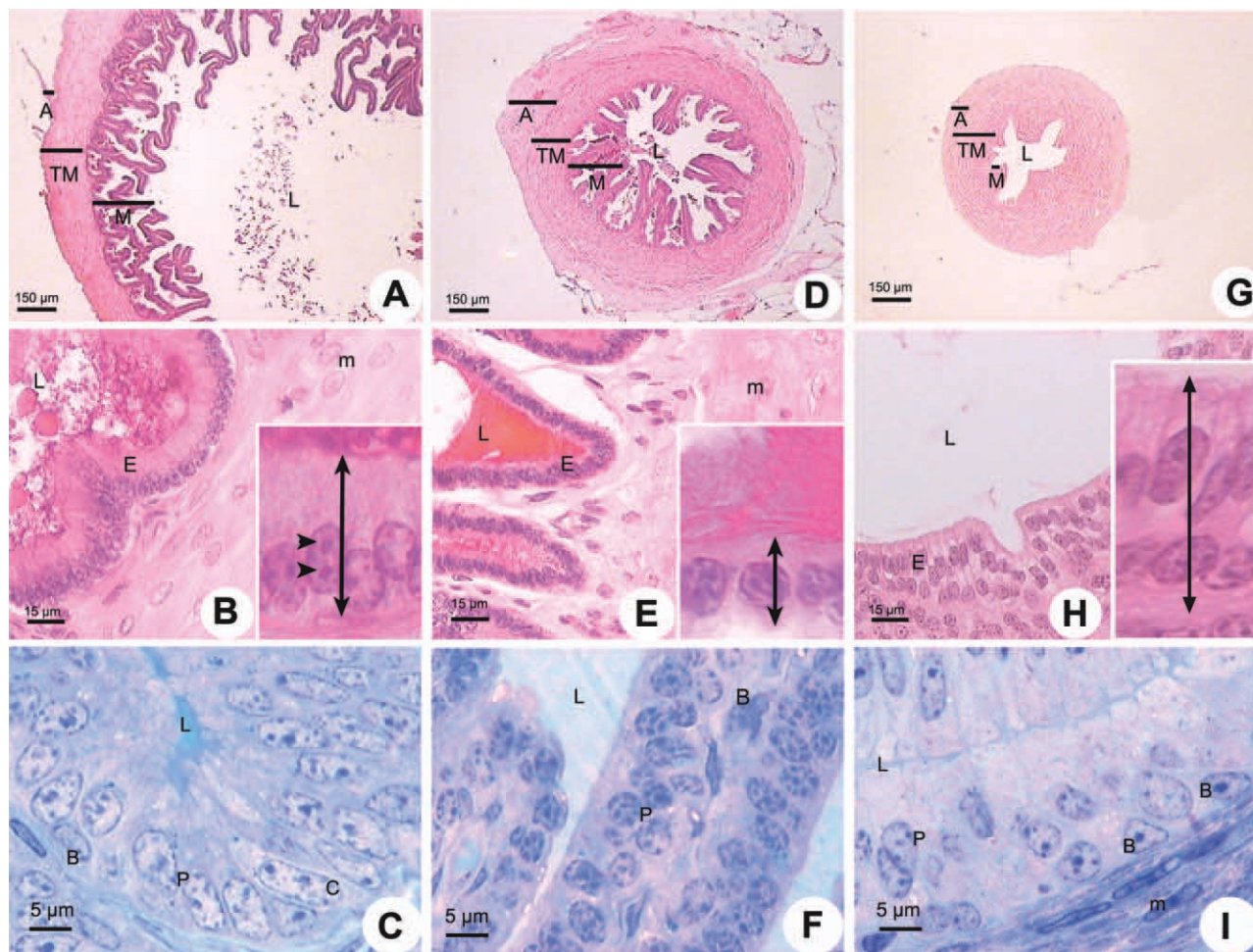
Fig. 1. Seasonal morphological variations and age-related changes of the seminal vesicle of viscacha. **A–C**: Period of activity. A: Image showing the radial disposition of the glandular histological layers. M, mucosa; TM, tunic muscle; A, adventitia; L, lumen. Hematoxylin-eosin. Scale bar: 150 μm. B: Pseudostratified cylindrical epithelium (E) of the gland. A thin muscular layer constituted by smooth muscle fibers (m) and collagen fibers is observed. L, lumen. Hematoxylin-eosin. Scale Bar: 15 μm. Inset: morphological characteristics of the nuclei of epithelial cells and epithelial height are observed at higher magnification. Arrowheads: nucleolus. C: Semithin sections showing principal cells (P) with elongated nuclei and moderately condensed chromatin, and evident nucleolus. Clear cell (C) present ovoid or elongated nuclei, lax chromatin, and poorly stained cytoplasm. B, basal cell; L, lumen. Toluidine blue. Scale Bar: 5 μm. **D–F**: Period of regression. D: In this image, a marked decrease in tubular diameter and epithelial height is observed. Note that epithelial folds of mucosa (M) are more extensive and irregular in relation to active period. TM, tunic muscle; A, adventitia; L, lumen. Hematoxylin-eosin. Scale Bar: 150 μm. E: Epithelial height shows a significant decrease. E, epithelium; m, smooth muscle fibers; Lu, lumen. Hematoxylin-eosin. Scale Bar: 15 μm. Inset: At higher magnification, morphological characteristics of the nuclei of epithelial cells and epithelial height are observed. F: In semithin sections, principal (P) and basal (B) cells show small nuclei with patches of condensed chromatin in associations with the nuclear envelope. L, lumen. Toluidine blue. Scale Bar: 5 μm. **G–I**: Impuber animals. G: Seminal vesicle image of an impuber animal showing significant variations in the structural parameters in relation to that observed in adult animals. M, mucosa; TM, tunic muscle; A, adventitia; L, lumen. Hematoxylin-eosin. Scale Bar: 150 μm. H: Note in this image a mucosa formed by scarce and irregular folds and a height pseudostratified epithelium (E). Inset details at high magnification, showing morphology of principal cells (P). L, lumen. Hematoxylin-eosin. Scale Bar: 15 μm. I: In semithin sections, principal cells with elongated nucleus, lax chromatin, and evident nucleolus are observed. Basal cells (B) of elongated shape with round or ovoid nucleus were localized in the epithelium base. L, lumen; m, muscular layer. Toluidine blue. Scale Bar: 5 μm.

Light Microscopy

In the period of maximum gonadal activity, the mucosa of the viscacha SV formed numerous folds lined with a simple cylindrical epithelium. The nuclei of the principal cells were elongated, had moderately condensed chromatin, an evident nucleolus, and were located perpendicularly to the lamina propria (Fig. 1B).

In the epithelium base, basal cells of elongated shape with a round or ovoid nucleus were observed. Semithin sections stained with toluidine blue allowed the identification of clear cells characterized by ovoid or elongated nuclei with lax chromatin and poorly stained cytoplasm. The lumen was large. A thin muscular layer, which constituted mainly by of smooth muscle fibers and collagen fibers, was found under the mucosa. A slender

TABLE 1. Structural parameters histological of the seminal vesicles in different periods reproductive and age of viscacha

Parameters (μm)	Activity	Regression	Impuber
Epithelial height*	16.95 ± 1.8[a]	11.25 ± 0.36	25.17 ± 1.12[b]
Mayor nuclear diameter*	6.16 ± 0.10[c]	5.24 ± 0.12	7.83 ± 0.11[d]
Luminal diameter	2,220–1,935	1,050–1,470	582–615
Muscular layer thickness*	160 ± 9.75[e]	318 ± 6.9	175 ± 6.37[f]

*The values are expressed as mean ± SEM ($n = 6$). The significant differences were determined by Student's t-test.
[a]$P < 0.001$: Activity versus regression.
[b]$P < 0.0001$: Impuber versus regression; impuber versus activity.
[c]$P < 0.001$: Activity versus regression.
[d]$P < 0.001$: Impuber versus regression; impuber versus activity.
[e]$P < 0.0001$: Activity versus regression.
[f]$P < 0.001$: Impuber versus regression

adventitia of loose connective tissue was located around these layers (Fig. 1A).

In the period of gonadal regression, the epithelial folds were more extensive and irregular when compared with the active period. A significant decrease in epithelial height was observed. The principal and basal cells both showed small nuclei with patches of condensed chromatin in association with the nuclear envelope. The lumen was markedly reduced and exhibited lower secretion levels (Fig. 1E,F).

The SVs in impuber viscachas were found also paired, but small and of whitish color. Few evaginations were observed in comparison to adult animals. Like in adults the SVs were tubular glands formed by three radially arranged histological layers: mucosa, muscular, and adventitia (Fig. 1G). The most striking characteristics were a mucosa formed by scarce and irregular folds of variable length and a glandular lumen showing a reduced luminal diameter with the absence of secretory products. The pseudostratified epithelium showed height cylindrical or cubic principal cells with an elongated nucleus, loose chromatin, and evident nucleolus (Fig. 1H,I). In the epithelium base, basal cells had an elongated shape and a round or ovoid nucleus. The muscular layers were well developed.

Changes in Luminal Diameter, Epithelial Height, and Muscular Layer Thickness During The Seasonal Reproductive Cycle. Differences Between Impuber and Reproductive Males

The analysis of these parameters in the SV corresponding to both periods is shown in Table 1. In the period of maximum gonadal activity, an increase of luminal diameter, epithelium height, and nuclear diameter of epithelial cells ($P < 0.001$) was observed. In contrast, the thickness of the muscular layer was thinner during the active period in comparison to gonadal regression (Figs. 1A–C and 1D–F).

In impuber animals, these parameters varied significantly. The luminal diameter was strongly reduced. The height of the glandular epithelium was higher and its nuclear diameters were greater than in the adult animal. The thickness of the muscular layer was intermediate in relation to the thickness measured performed in adult animals during periods of activity and regression (Fig. 1G–I).

Electron microscopy

In the active period, principal, clear, and basal cells were observed (Fig. 2A,B). Principal cells ranged from the basal membrane to the luminal surface of the epithelium and were cubic or columnar with regular edges, lax chromatin, and evident nucleoli. They had a wide cytoplasmic apical surface, and, in the basal region, thin cytoplasmic processes seem to come into contact with the epithelial basement membrane. In their luminal surface, we observed abundant microvilli. The cytoplasms contained numerous mitochondria and a well-developed rough endoplasmic reticulum (RER) and were mainly localized in the supranuclear region of the principal cells. The RER had expanded cisterns, and we observed ovoid or elongated mitochondria and scarce clear vacuoles (Fig. 2C). Cytoplasmic protrusions in the apical region indicated an apocrine secretion. Clear cells extended from the basal membrane toward the lumen in a form similar to that described for principal cells. These columnar cells had basal nuclei and moderately lax chromatin. The cytoplasm was less electron dense than that of principal cells and was characterized by scarce presence of RER and absence of Golgi apparatus (Fig. 2B). Basal cells were located in the basal region of the epithelium. They possessed a lax round nuclei and a narrow cytoplasm with few content of organelles. The basal cells were small and projected narrow cytoplasmic extensions between the principal cells that never reached the luminal surface (Fig. 2A).

During the period of gonadal regression, the same cell types were observed, but exhibited a marked reduction in size and content of organelles. Principal columnar cells showed different stages of maturation (Fig. 2D). The nuclei of these cells were round or oval with irregular and heterochromatic edges (Fig. 2E). RER and Golgi complex showed altered cisterns (Fig. 2F). Few mitochondria were observed. In the apical cytoplasm of clear cells, numerous vacuoles and altered mitochondria were found. In the principal and clear cells, dense bodies and glycogen granules with varying diameters and different shapes were observed (Fig. 2E,F).

In impuber viscachas, principal and basal cells are the main two cell types that could be distinguished at this age (Fig. 3A). Similar to observations in adult animals, the principal cells were columnar. The nucleus of these cells was large, oval in shape with regular edges, and
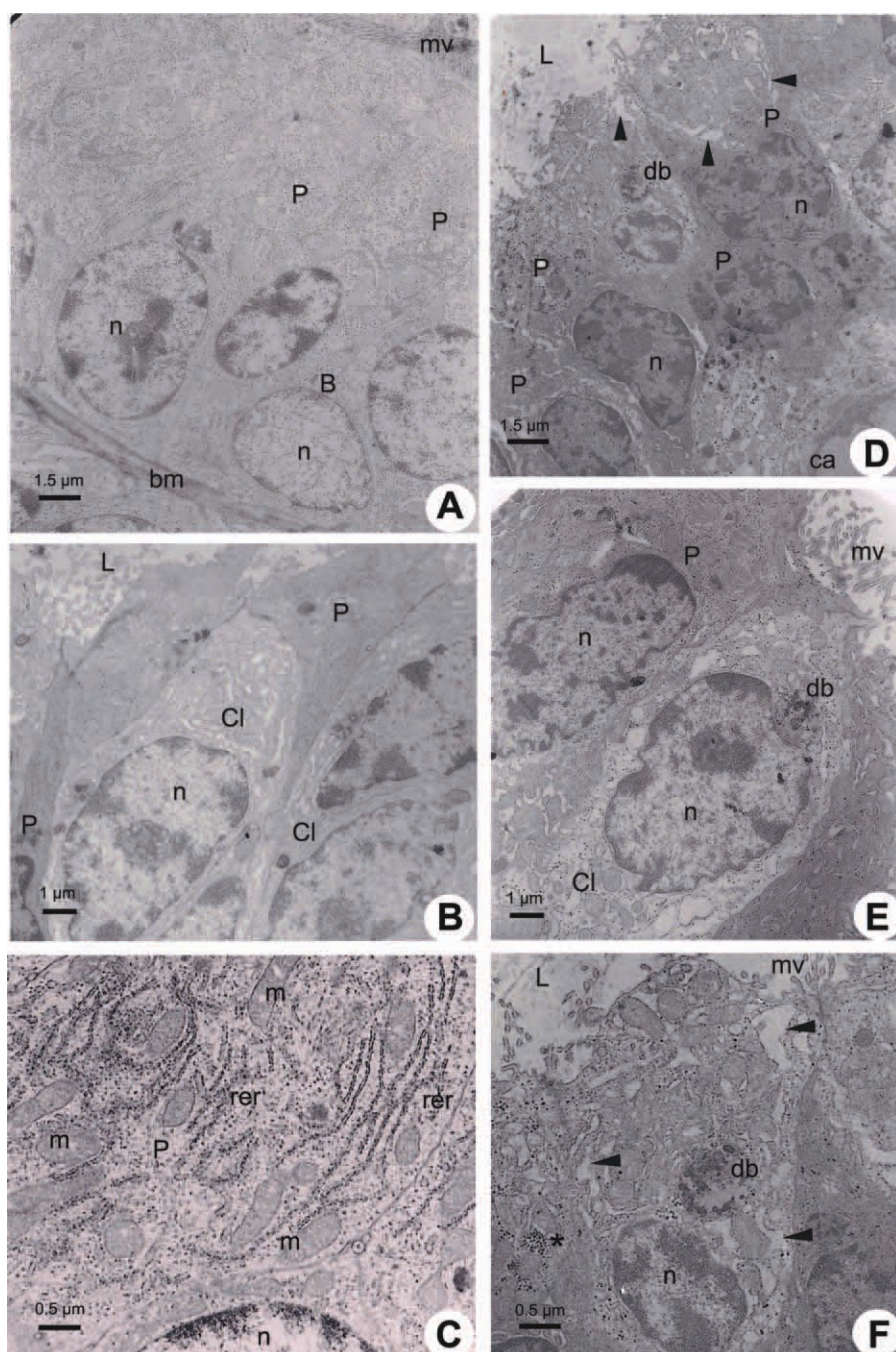
Fig. 2. Transmission electron microscopy of seminal vesicle of adult viscacha. **A–C**: Period of activity. A: Image showing the disposition of the principal (P) and basal (B) cells. In P cells, observe a wide cytoplasmic apical surface with abundant microvilli (mv). Nuclei (n) of principal and basal (B) cells show irregular edges and lax chromatin. bm, basal membrane. Scale bar: 1.5 μm. B: Clear (Cl) cells extend from the basal membrane toward the lumen. Observe the different electronic densities among the cytoplasms of the clear and principal (P) cells. n, nucleus; L, lumen. Scale bar: 1 μm. C: Cytoplasm of the supranuclear region of principal (P) cells showing abundant mitochondria (m) and well-developed rough endoplasmic reticulum (rer). n, nuclei. Scale bar: 0.5 μm. **D–F**: Period of regression. D: Principal (P) cells with irregular nuclei (n) and variable sizes are observed. db, dense bodies; L, lumen; ca, capilar. Scale bar: 1.5 μm. E: In this image, principal (P) and clear (Cl) cells show nuclei with irregular edges and variable shapes. Dense body (db) near the nucleus (n) of the clear cell is observed. mv, microvilli. Scale bar: 1 μm. F: Apical region of cytoplasm of principal (P) cell showing dilated cisterns of rough endoplasmic reticulum (arrow). Dense body (db) and glycogen granules (asterisk) with variable shape are observed. n, nuclei; mv, microvilli; L, lumen. Scale bar: 0.5 μm.
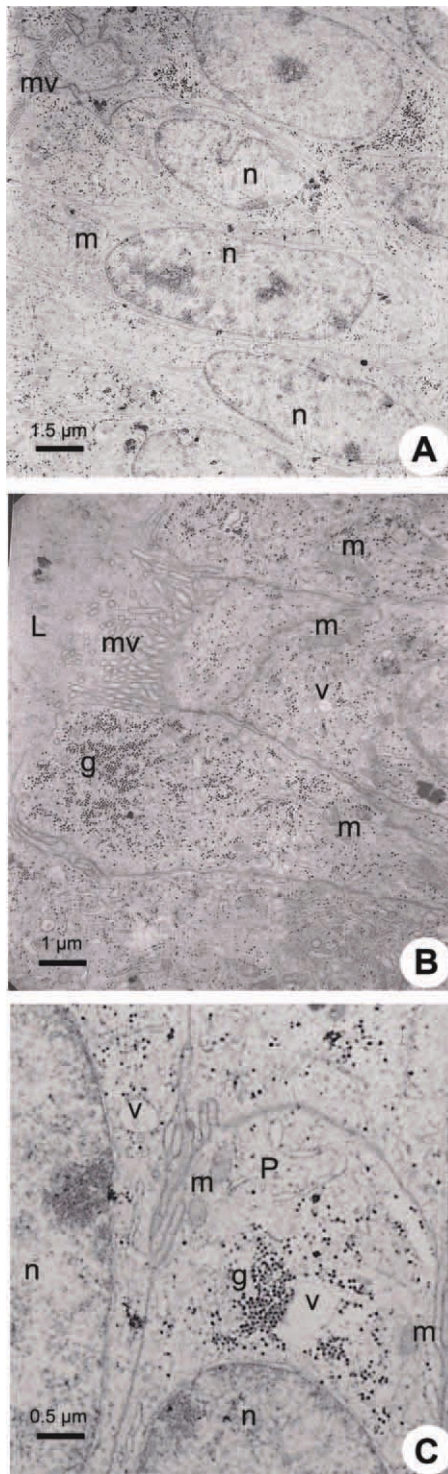
Fig. 3. Transmission electron microscopy of seminal vesicle of impuber viscacha. **A**: Image showing principal cells with large nuclei (n) of oval shape and regular edges. m, mitochondria; mv, microvilli. Scale bar: 1.5 μm. **B**: Supranuclear region of principal cell. Note the presence of vacuoles (v) and abundant granules of glycogen (g). m, mitochondria; mv, microvilli; L, lumen. Scale bar: 1 μm. **C**: Details at higher magnification showing the storage glycogen (g) in the principal cells (P) and its relationship with vacuoles (v). n, nucleus; m, mitochondria. Scale bar: 0.5 μm.

was located in the third basal of cellular cytoplasm. The chromatin was lax and had one or more compact nucleoli. The large and slightly stained cytoplasm contained small mitochondria, a poorly developed Golgi apparatus, and a large number of free ribosomes. In the supranuclear region of these cells, various forms of numerous small vesicles and granules of glycogen were observed (Fig. 3B,C). The basal cells are small pyramidal cells that never reached the luminal surface. They were located between the narrow basal extensions of the principal cells. They possessed lax round nuclei and a narrow peripheral cytoplasmic rim with few organelles.

Testosterone

Seasonal variations and age-related changes of serum testosterone levels are shown in Table 2. During the active period, adult animals showed elevated levels of serum testosterone (490.66 ± 40.76 ng/dL), whereas in the period of regression the results showed a marked decrease in testosterone (127.66 ± 14.31 ng/dL) similar to that observed in impuber animals (118.23 ± 10.56 ng/dL).

Immunohistochemistry

In adult animals, the percentage of AR-immunoreactive cells exhibited seasonal variations through the annual reproductive cycle (Table 2). In the period of gonadal regression, the percentage of AR-immunolabeled cells was incremented significantly ($P < 0.0001$), in relation to the period activity values.

In active period, ARs were located in the nuclei of epithelial cells and expressed a weak immunostaining (Fig. 4A). However, in the stroma, fibroblasts and smooth muscle cells showed a moderate immunoreactivity (Fig. 4B).

During the gonadal regression period, the gland mucosa exhibited numerous epithelial cells with intense nuclear staining. Cells of the fibromuscular stroma were weakly positive to AR (Fig. 4C,D).

In impuber animals, there was a high percentage of AR-immunolabeled cells similar to that observed in the regression period in adult male animals (Table 2). In the connective tissue, a moderate immunolabeling for AR was observed in the nuclei of the muscular cells (Fig. 4E,F).

DISCUSSION

In photoperiod-dependent rodents, the pineal melatonin is known by its antigonadotropic function, which causes a decrease in LH and FSH, and a fall in testosterone levels that lead to a consequent decrease in gonadal function (Zieba et al., 2008). Numerous morphological studies have been carried out on SVs in different experimental animal models. Nevertheless, studies referring to cyclic variations in the SVs of wild animals are scarce.

In this study, we use the light and electronic microscope to achieve a better understanding of the SV physiology in the seasonal cyclic reproduction of this rodent. We also determined the serum testosterone levels in different stages of reproductive cycle and in relation to age. Furthermore, we studied the location of

TABLE 2. Seasonal variations in serum testosterone, percentage and distribution of cells immunolabeled for AR in adult and impuber male viscachas (*Lagostomus maximus maximus*)

	Activity	Regression	Impuber
Serum testosterone (ng/dL)	490.66 ± 40.76[a]	127.66 ± 14.31	118.23 ± 10.56
% Immunopositive cells	43.3% ± 2.5%[b]	80.21% ± 0.39%	74.76% ± 0.24%
Epithelial cells	+	+++	+++
Stromal fibromuscular cells	++	+	++

Staining intensity scores were as follows: +, weak; ++, moderate; +++, intense.
The values are expressed as mean ± SEM ($n = 6$). Significant differences were determined by Student's *t*-test.
[a]$P < 0.0001$: Activity versus regression; activity versus impuber.
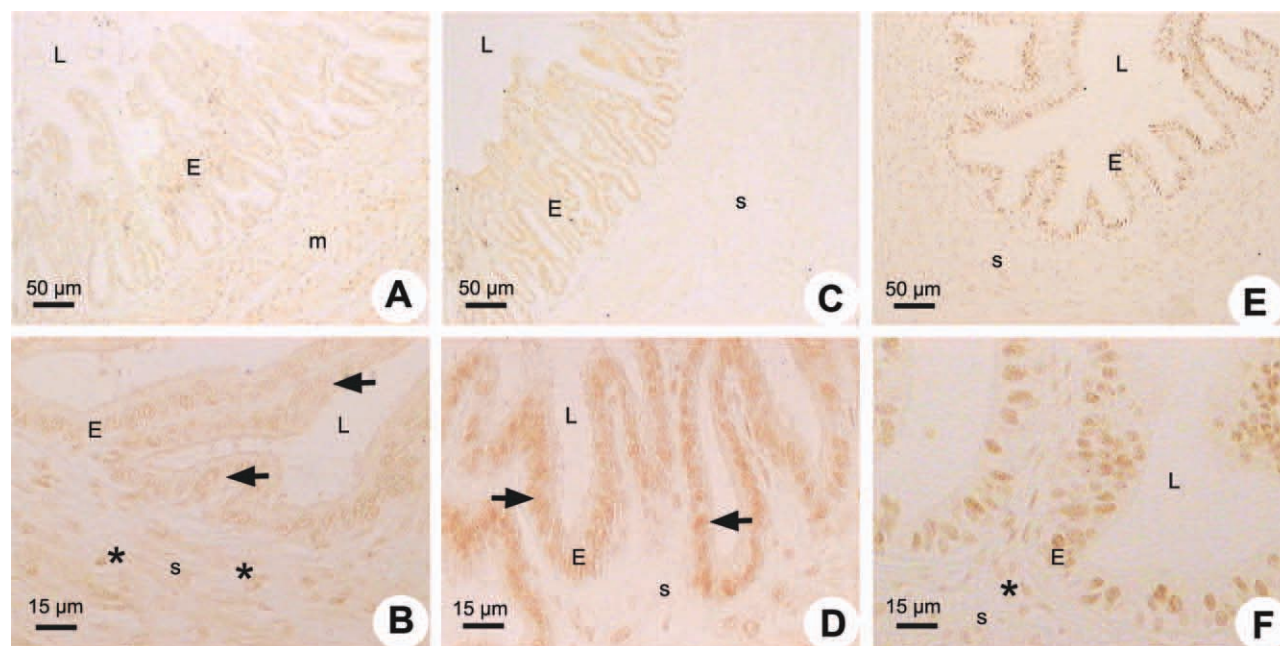[b]$P < 0.001$: Activity versus regression; activity versus impuber.

Fig. 4. Immunohistochemistry for androgen receptors in seminal vesicles of viscacha. **A** and **B**: Period of activity. A: Image showing a weak immunostaining in the glandular epithelium (E). L, lumen. Scale bar: 50 μm. B: At higher magnification, this image shows nuclei of the epithelial cells (arrows) with weak immunostaining. The moderately immunolabeled cells are observed in fibroblasts and smooth muscle cells (asterisk) of stroma (s). E, epithelium; L, lumen. Scale bar: 15 μm. **C** and **D**: Period of regression. C: Image showing glandular mucosa with epithelial cells (E) intensely immunolabeled. L, lumen; s, stroma. Scale bar: 50 μm. D: In this image, nuclei of epithelial cells show intensive immunostaining (arrows). E, Epithelium; L, lumen; s, stroma. Scale bar: 15 μm. **E** and **F**: Impuber animals. E: Note in this image, the strong immunostaining in the epithelial cells (E). s, stroma. Scale bar: 15 μm. F: In the stroma (s), a moderate immunostaining for androgen receptor was observed in the nuclei of the muscular cells (asterisk). L, lumen. Scale bar: 15 μm.

ARs by immunohistochemistry for this gland during both periods and in impuber animals.

Our results demonstrate that the structure of the SVs changes during the seasonal reproductive cycle of viscacha. Specifically, the morphometric analysis of luminal diameter and epithelial height allowed us to confirm that these parameters show a significant increment during the reproductive active period when compared with the regression period. The epithelial cells presented nuclei with evident nucleolus. These changes are probably due to elevated levels of testosterone leading to an increase in the secretory activity of epithelial cells and a great storage of secretion into the glandular lumen.

On the other hand, our results demonstrate that the secretory epithelium of viscacha SVs is lined by three types of cells: principal, clear, and basal. The major ul-

trastructural changes were observed in the principal cells. During the regression period, these cells exhibit signs of diminished cellular activity characterized by cytoplasmic reduction, presence of irregular nuclei, dilated cisterns (RER), and altered mitochondria. These ultrastructural changes correlate with a decrease in luminal diameter and decreased serum testosterone levels, which allow us to postulate a decrease in the protein synthesis activity of SVs, in agreement with the observations of Gernigon et al. (1994) in Saharian rodent. On the other hand, in the sexually active period, the principal cells are rich in RER and ribosomes. The great development of the RER indicates an intense activity of protein synthesis in the columnar cells. Protein synthesis consumes at least four high-energy phosphate bonds (Alberts et al., 2002) and, thus, a great amount of ATP.

This high energetic expense may explain the abundance of mitochondria in the cytoplasm of principal cells.

The principal and basal cells, but not the clear cells, have been previously reported in the SVs of goats (Wrobel, 1970), bulls (Amselgruber and Feder, 1986), and humans (Riva and Aumuller, 1994). However, Badia et al. (2006) described the presence of clear cells of boar SVs, in agreement with our observations in viscacha. Therefore, this allows us to postulate that principal cells of the SVs may be functionally differentiated cells, whereas the clear cells without secretory granules and with poorly developed RER found in viscacha might correspond to an initial stage of differentiated columnar cells.

The basal cells are scarce and characterized by the presence of few organelles and the absence of secretory granules. The exact function of these cells in the epithelium is still unclear. Basal cells could act as potential mediators between luminal cell and stromal cell activity by regulating material secretion (El-Alfy et al., 2000). In addition, basal cells have also been postulated to have a structural role (Hayward et al., 1996) and to serve as reserve or stem cells of the columnar cells (Verhagen et al., 1988; Riva and Aumüller, 1994).

In the SVs of impuber animals, observations with TEM showed that the gland epithelium was formed by cells similar to those described in adult animals during the gonadal regression period. The epithelial cells of impuber animals exhibited poor organelle development, as well as abundant vesicles and small glycogen granules, accumulated in the apical region. In these cells, the nuclei morphology was characteristic of intense activity, whereas in regressed adult males signs corresponding to cellular atrophy were observed.

The immunohistochemical study in *Lagostomus maximus maximus* demonstrates variations in the distribution of AR in the gland as well as changes in immunostaining/labeling throughout the reproductive cycle. In the regressive period, a higher percentage of AR-immunolabeled cells were observed in the epithelial cells nucleus, and connective tissue cells exhibited weak immunolabeling. Taking into consideration that during the period of gonadal regression and in impuber animals the testosterone values are lowest, our immunohistochemical results demonstrate a significant correlation with the percentage of AR-immunopositive cells. These data agree with observations by Li-Xin et al. (1990) and Blok et al. (1992), who found decreased levels of serum testosterone and increased levels of AR expression after performing chirurgical and chemical castration techniques. This allows us to hypothesize that the expression of AR is increased when the levels of the androgenic hormone are low to maintain the gland normal functioning.

Morphological variations found in the viscacha SVs were correlated with results previously obtained in our laboratory for the testicle and epididymis of this rodent. A study conducted by Muñoz et al. (1998) demonstrated that testicular histology has a significant decrease in the seminiferous tubule diameter and in the number of layers of germinal cells seasonally period, along with structural changes in Sertoli and Leydig cells (Muñoz et al., 1997, 2001). On the other hand, Aguilera-Merlo et al. (2005a, 2009) found in the epididymal morphological changes during the reproductive cycle of viscacha. Specifically, the morphometric analysis of luminal diameter, epithelial height, and thickening of lamina propria

allowed us to confirm that these parameters present significant seasonal variation mainly in the cauda.

Our findings in *Lagostomus* revealed higher testosterone serum levels in the activity period compared with the period of regression. The fall of testosterone and the hypotrophy of Leydig cells, caused by a decrease of the testicular sensitivity to LH stimulation, would be one of the factors responsible for gonadal regression in this rodent. Furthermore, the photoperiod variations, through pineal hypothalamus pituitary axis and the hormone melatonin, would represent the principal primary signal responsible for the cyclical breeding activity in viscacha.

In conclusion, the results presented in this work indicate that the SVs of *Lagostomus maximus maximus* experience changes throughout the annual reproductive cycle. This allows us to postulate that the SVs may be influenced by the same hormonal changes observed in the gonads and the epididymal tract, which are closely related to variations of the natural photoperiod.

LITERATURE CITED

Aguilera-Merlo C, Fogal T, Sator T, Dominguez S, Sosa M, Scardapane L, Piezzi R. 2009. Ultrastructural and biochemical seasonal changes in epididymal corpus and cauda of viscacha (*Lagostomus maximus maximus*). J Morphol 270:805–814.

Aguilera-Merlo C, Muñoz E, Dominguez S, Scardapane L, de Rosas JC. 2005b. Seasonal variations in the heterologous binding of viscacha spermatozoa. A scanning electron microscope study. Biocell 29:243–251.

Aguilera-Merlo C, Muñoz E, Dominguez S, Scardapane L, Piezzi R. 2005a. Epididymis of viscacha (*Lagostomus maximus maximus*). Morphological changes during the annual reproductive cycle. Anat Rec 282:83–92.

Alberts B, Bray D, Lewis J, Raff M, Roberts K, Watson JD. 2002. Molecular biology of the cell. New York: Garland Publishing. 1463p.

Amselgruber W, Feder FH. 1986. Licht- und elektronenmikroskopische untersuchugen der samenblasendrüse (*Glandula vesicularis*) desbullen. Anat Histol Embryol 15:361–379.

Ayres de Menezes DJ, Assis Neto AC, Oliveira MF, Miglino MA, Pereira GR, Ambrósio CE, Ferraz MS, Carvalho MA. 2010. Morphology of the male agouti accessory genital glands (*Dasyprocta prymnolopha* Wagler, 1831). Pesq Vet Bras 30:793–797.

Badia E, Briz M, Pinart E, Garcia-Gil N, Bassols J, Pruneda A, Bussalleu E, Yeste M, Casas I, Bonet S. 2006. Structural and ultrastructural feature of boar seminal vesicles. Tissue cell 38:79–91.

Blok LJ, Bartlett JM, Bolt de Vries J, Themmen AP, Brinkmann AO, Weinbauer GF, Nieschlag E, Grootegoed JA. 1992. Effect of testosterone deprivation on expression of the androgen receptor in rat prostate, epididymis and testis. Int J Androl 15:182–198.

Branch LC, Villarreal D, Fowler GS. 1993. Recruitment, dispersal, and group fusion in a declining population of the plains vizcacha (*Lagostomus maximus maximus;* Chinchilidae). J Mammal 74:9–20.

Dellman HD. 1993. Histología veterinaria, 2nd ed. Zaragoza: Acribia. p 398.

Demas GE, Polacek KM, Durazzo A, Jasnow AM. 2004. Adrenal hormones mediate melatonin-induced increases in aggression in

male Siberian hamsters (*Phodopus sungorus*). Horm Behav 46: 582–591.

Dominguez S, Piezzi R, Scardapane L, Guzmán J. 1987. A light and electron microscopic study of the pineal gland of the viscacha (*Lagostomus maximus maximus*). J Pineal Res 4:211–219.

El-Alfy M, Pelletier G, Hermo LSF. 2000. Unique features of the basal cells of human prostate epithelium. Microsc Res Tech 51: 436–446.

Filippa V, Penissi A, Mohamed F. 2005. Seasonal variations of gonadotropins in the pars distalis male viscacha pituitary. Effect of chronic melatonin treatment. Eur J Histochem 49:291–300.

Fuentes L, Calvo JC, Charreau E, Guzman J. 1993. Seasonal variations in testicular LH, FSH and Prl receptors; in vitro testosterone production and serum testosterone concentration in adult male viscacha (*Lagostomus maximus maximus*). Gen Comp Endocrinol 90:133–141.

Fuentes L, Caravaca N, Pelzer L, Scardapane L, Piezzi R, Guzmán R. 1991. Seasonal variations in the testis and epididymis of viscacha (*L.m.m.*). Biol Reprod 45:493–497.

Garidou ML, Roels BV, Pévet P, Miguez P, Simonneaux V. 2003. Mechanism regulating the marked seasonal variation in melatonin synthesis in the European hamster pineal gland. Am J Physiol 284:1043–1052.

Gernigon T, Berger M, Lécher P. 1994. Seasonal variations in the ultrastructure and production of androgen-dependent proteins in the seminal vesicles of a Saharian rodent (*Psammomys obesus*). J Endocrinol 142:37–46.

Hayward SW, Brody JR, Cunha GR. 1996. An edgewise look at basal epithelial cells: three-dimensional views of the rat prostate, mammary gland and salivary gland. Differentiation 60:219–227.

Jackson J. 1989. Reproductive parameters of the plains viscacha (*Lagostomus maximus maximus*) in San Luis province, Argentina. Vida Silvestre Neotropical 2:57–62.

Jackson JE, Branch LC, Villarreal D. 1996. *Lagostomus maximus*. Mammalian Species 543:1–6.

Karnovsky MJ. 1965. A formaldehyde-glutaraldehyde fixative of high osmolarity for use in electron microscopy. J Cell Biol 27: 137A–138A.

Li-Xin S, Rodriguez MC, Jänne OA. 1990. Regulation of androgen receptor protein and mRNA concentrations by androgens in rat ventral prostate and seminal vesicles and in human hepatoma cells. Mol Endocrinol 4:1636–1646.

Llanos A, Crespo J. 1954. Ecología de la vizcacha (*Lagostomus maximus maximus*) en el nordeste de la provincia de Entre Ríos. Revista de Investigaciones Agrícolas. Extra Nueva Serie 10:5–95.

Luke M, Coffey D. 1994. The male sex accessory tissue. Structure, androgen, action, and physiology. In: Knobil E, Neil J, editors. The physiology of reproduction. New York: Raven Press. p 1435–1487.

Mahendroo MS, Cala KM, Hess DL, Russel DW. 2001. Unexpected virilization in male mice lacking steroid 5α-reductase enzymes. Endocrinology 142:4652–4662.

Meyer L, Caston J, Mensah-Nyagan AG. 2006. Seasonal variation of the impact of a stressful procedure on open field behaviour and blood corticosterone in laboratory mice. Behav Brain Res 167: 342–348.

Mohamed F, Fogal T, Dominguez S, Scardapane L, Guzmán J, Piezzi R. 2000. Colloid in the pituitary pars distalis of viscacha (*Lagostomus maximus maximus*): ultrastructure and occurrence in relation to season, sex, and growth. Anat Rec 258:1–10.

Mollineau WM, Adogwa AO, Garcia GW. 2009. The gross and micro anatomy of the accessory sex glands of the male agouti (*Dasyprocta leporina*). Anat Histol Embryol 38:204–207.

Muñoz E, Fogal T, Dominguez S, Scardapane L, Guzmán J. 2001. Ultrastructural and morphometric study of the Sertoli cell of the viscacha (*Lagostomus maximus maximus*) during the annual reproductive cycle. Anat Rec 262:176–185.

Muñoz E, Fogal T, Dominguez S, Scardapane L, Guzmán J, Piezzi R. 1997. Seasonal changes of the Leydig cells of viscacha (*Lagostomus maximus maximus*). A light and electron microscopy study. Tissue Cell 29:119–128.

Muñoz E, Fogal T, Dominguez S, Scardapane L, Guzmán J, Piezzi R. 1998. Stages of the cycle of the seminiferous epithelium of the viscacha (*Lagostomus maximus maximus*). Anat Rec 252:8–16.

Riva A, Aumüller G. 1994. Epithelium of the distal portion of the human spermatic pathway: seminal vesicle, ampulla ductus deferentis and ejaculatory duct. In: Motta PM, editor. Ultrastructure of the male urogenital glands: prostate, seminal vesicles, urethral, and bulbourethral glands. New York: Kluwer Academic Publisher. p 35–49.

Setchell BP, Maddocks S, Brooks DE. 1994. Anatomy, vasculature, innervations, and fluids of the male reproductive tract. In: Knobil E, Neill JD, editors. The physiology of reproduction. New York: Raven Press. p 1063–1175.

Strzezek J, Martín-Rillo S, i Sáiz-Cidoncha F. 2000. Glándula vesicular seminal del verraco: su papel en la capacidad de fertilización. Anaporc 205:59–84.

Thompson A. 2001. Role of androgen and fibroblast growth factors in prostatic development. Reproduction 121:187–195.

Verhagen AP, Aalders TW, Ramaekers FC, Debruyne FM, Schalken JA. 1988. Differential expression of keratins in the basal and luminal compartment of rat prostatic epithelium during degeneration. Prostate 13:25–38.

Welsh M, Saunders PT, Marchetti NI, Sharpe RM. 2006. Androgen-dependent mechanisms of Wolffian duct development and their pertubation by flutamide. Endocrinology 147:4820–4830.

Wrobel KH. 1970. Zur morphologie des samenblasenepithels der ziege. Zentralbl Veterinarmed A 17:634–643.

Zieba DA, Szczesna M, Klocek-Gorka B, Molik E, Misztal T, Williams GL, Romanowicz K, Stepien E, Keisler DH, Murawski M. 2008. Seasonal effects of central leptin infusion on secretion of melatonin and prolactin and on SOCS-3 gene expression in ewes. J Endocrinol 198:147–155.